

A NEW ELECTROMAGNETIC INSTRUMENT FOR THICKNESS GAUGING OF CONDUCTIVE MATERIALS

J. P. Fulton, B. Wincheski, and S. Nath
Analytical Services and Materials, Inc.
107 Research Drive
Hampton, VA 23666

J. Reilly, and M. Namkung
NASA, Langley Research Center
Hampton, VA 23681

INTRODUCTION

Eddy current techniques are widely used to measure the thickness of electrically conducting materials [1-3]. The approach, however, requires an extensive set of calibration standards and can be quite time consuming to set up and perform. Recently, an electromagnetic sensor was developed which eliminates the need for impedance measurements [4-8]. The ability to monitor the magnitude of a voltage output independent of the phase enables the use of extremely simple instrumentation. Using this new sensor a portable hand-held instrument was developed (Fig. 1). The device makes single point measurements of the thickness of nonferromagnetic conductive materials. The technique utilized by this instrument requires calibration with two samples of known thicknesses that are representative of the upper and lower thickness values to be measured. The accuracy of the instrument depends upon the calibration range, with a larger range giving a larger error. The measured thicknesses are typically within 2-3% of the calibration range (the difference between the thin and thick sample) of their actual values. In this paper the design, operational and performance characteristics of the instrument along with a detailed description of the thickness gauging algorithm used in the device are presented.

DESIGN AND OPERATIONAL CHARACTERISTICS OF THE PROBE

For completeness a brief overview of the basic operating characteristics of the probe is presented. A more detailed description of how the probe works can be found elsewhere [4-6]. The unique feature of the probe is the presence of a ferromagnetic cylinder (sometimes called a shield or a lens) between the drive and the pickup coil (Fig. 2A). When the operating frequency of the probe is sufficiently high the instrument produces a large signal when the probe is held in air, but a negligible output when placed on a conducting sample (Fig. 2B). This phenomenon is due to the ferromagnetic shield which focuses the magnetic flux in a ring around the pickup coil. A series of axisymmetric finite element models were created

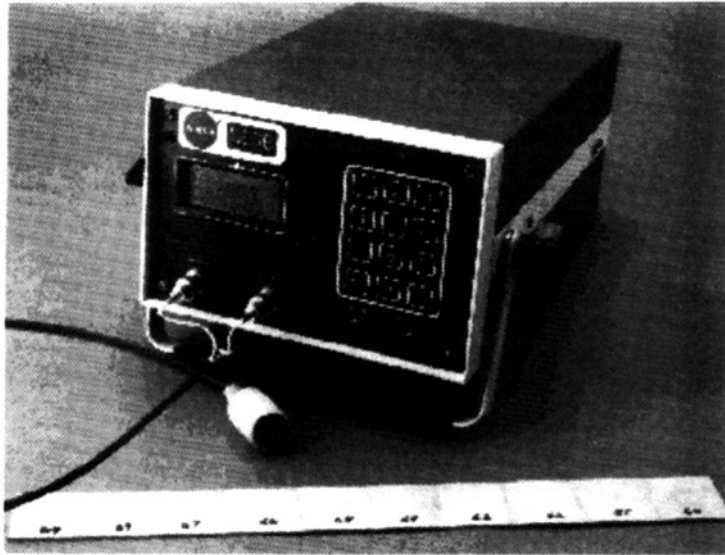


Fig. 1. Photograph of electromagnetic thickness gauging instrument.

to study this phenomenon and the results are displayed in Figs. 3 & 4 below. The ring of flux induces eddy currents in the test sample which, together with the shield, isolate the pickup coil from the drive coil. As the drive frequency is reduced the probe no longer provides a null voltage. The flux from the drive coil passes through the sample and begins to link with the pickup coil as shown in Fig. 4.

The magnitude of the induced voltage is proportional to both the conductivity and thickness of the sample. Experimental results showing the probe output as a function of frequency for aluminum samples of varying thickness is shown in Fig. 5. The variation in probe output with thickness has been used to qualitatively monitor material loss in conductive samples. Fig. 6 shows the results of a c-scan image of the probe response for interlayer corrosion damage. Corrosion was simulated by mechanically removing material from the back surface of the top panel of two 1.6 mm aluminum plates. Material losses in the shape of an "N" ranging from 1.5 - 6.0% were detected with the probe operating at 2.5kHz.

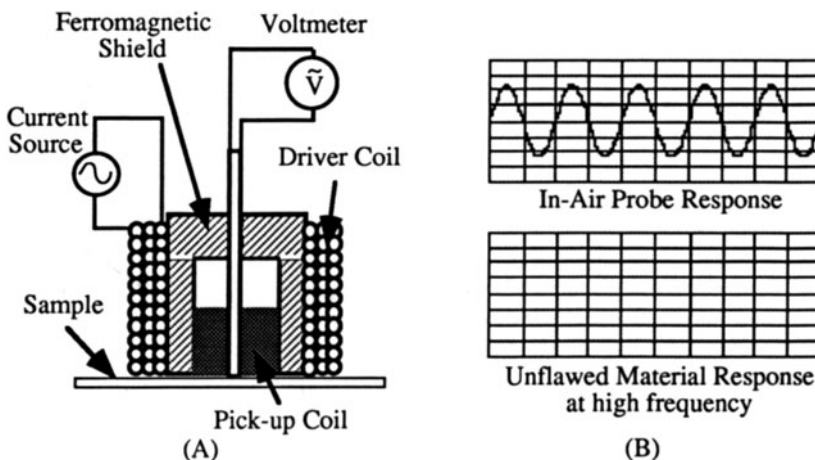


Fig. 2. Schematic of probe design and typical probe outputs.

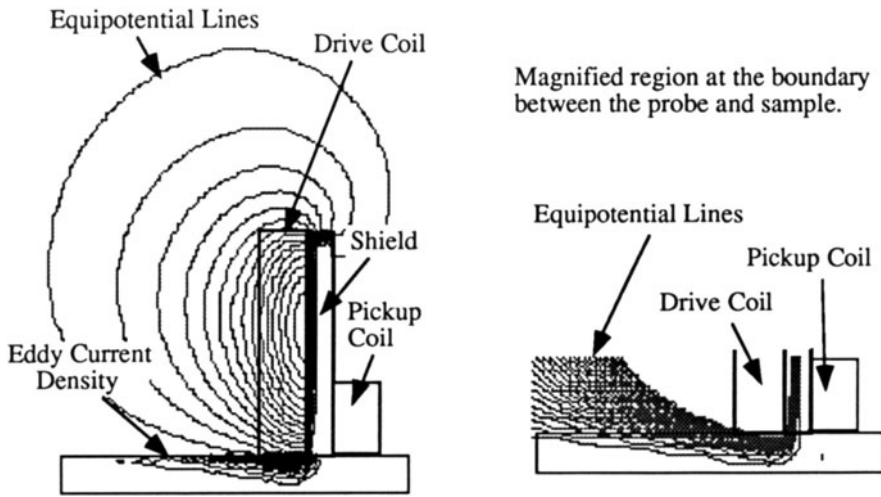


Fig. 3. Axisymmetric finite element modeling results showing eddy currents and lines of flux for the electromagnetic probe operating at 70kHz.

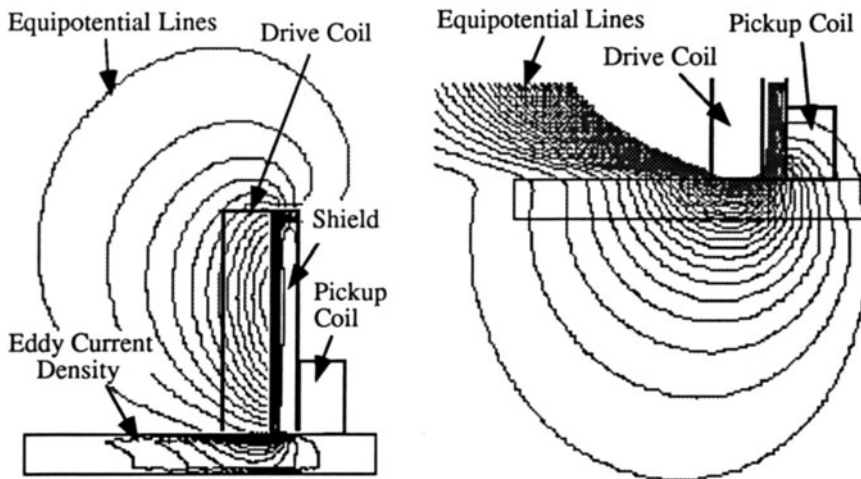


Fig. 4. Axisymmetric finite element modeling results showing eddy currents and lines of flux for the electromagnetic probe operating at 7kHz.

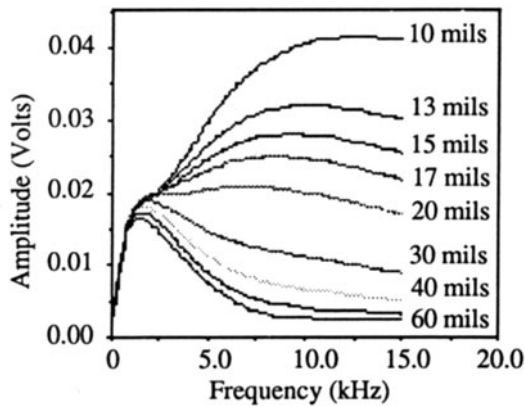


Fig. 5. Probe response as a function of drive frequency and material thickness.

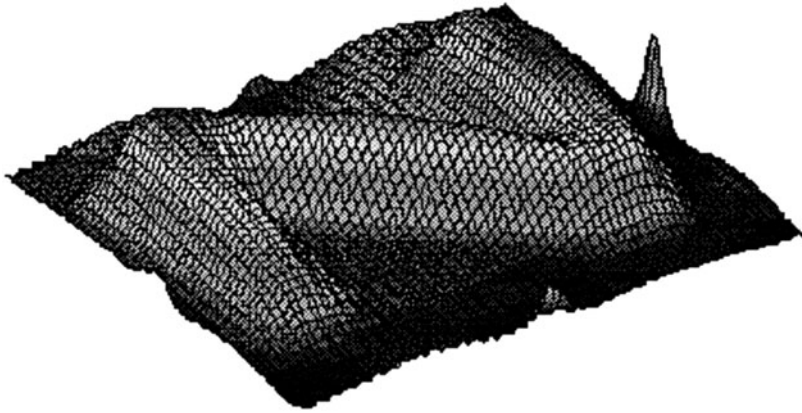


Fig. 6. C-scan image of manufactured corrosion sample at 2.5kHz.

If the drive frequency is reduced even further, flux produced by the drive coil begins to pass directly through the ferromagnetic shield and link with the pickup coil. A schematic illustration of the flux penetrating the shield and linking with the pickup coil is shown in Fig. 7 below. This flux is in addition to flux passing through the sample as discussed previously. The behavior is unwanted since the magnitude of the induced voltage is now also dependent on the conductivity and thickness of the shield and not just the sample. Thus, for low frequency operation the thickness, permeability, and the conductivity of the shield become very important and should be chosen to reduce the direct fields from the drive coil. We are measuring relatively small fields, consequently, the magnitude of the direct fields from the drive coil needs to be very small. To reduce the flux passing directly through the shield, the shields permeability, conductivity and thickness must be chosen carefully. Two suitable materials are 1020 steel and mu-metal. Both have similar electrical conductivities, but the permeability of mu-metal is approximately two orders of magnitude higher than the steel. The higher permeability allows for a much thinner shield with mu-metal than is possible with the steel. This is desirable since the overall dimensions of the probe can be reduced and more localized measurements can be made. The only disadvantages of mu-metal is its expense and its toughness for machining.

THICKNESS GAUGING ALGORITHM

An algorithm for using the new electromagnetic probe to determine the thickness of a

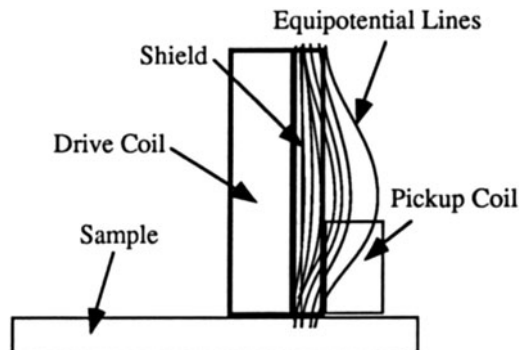


Fig. 7. Schematic illustration of flux passing directly through the shield and linking with the pickup coil.

sample should meet certain criteria. It must be easy to use, able to provide accurate and repeatable results and it should be fairly robust, i.e. applicable over a “wide” range of thickness variations. As is the case for all other single sided thickness gauging techniques, a set of calibration standards will also be required with this probe. This is due to the conductivity dependence of the probe output voltage. A major emphasis will be placed on making the calibration as simple as possible for the user.

The relationship between the output of the probe and both the thickness of the sample and the frequency of the drive coil is nonlinear, as shown in Fig. 5 above. Both of the nonlinearities will have a significant impact on our technique. To obtain a sufficient level of accuracy there are two possible options for devising a calibration algorithm. Either a piecewise linear interpolation scheme can be employed or the nonlinearity can be accounted for directly by using nonlinear interpolation. The major drawback of using a piecewise linear approximation is that the calibration range would have to be relatively small. As a result, a rather extensive set of calibration standards would be required and testing would become rather tedious and cumbersome. A nonlinear approach, on the other hand, would have an increased range of applicability for a given set of standards and a less complicated calibration procedure for the end user. It will, however, require instrumentation with slightly more computational capabilities.

Another difficulty with quantifying the results over a wide range of thicknesses is the dependence of thickness separation on the drive frequency. Higher frequencies are better for separating out the thinner samples, while thicker samples need information from the lower frequencies for a reasonable degree of separation. Consequently, the “ideal” frequency with which to inspect a particular sample would need to be determined before testing. Since this would unnecessarily complicate the testing an alternative approach was investigated.

To enable a wider measurement range without requiring any a priori knowledge by the user, results from many frequencies instead of using only a single frequency measurement were used. It was discovered that integrating the probe output as we sweep through a suitable range of frequencies will yield a unique value depending upon the thickness and conductivity of the sample. A typical integrated signal is shown schematically in Fig. 8A below, where the area highlighted by the shaded region is unique for each sample thickness. When this integrated probe output is plotted as a function of the sample thickness, the results fit very nicely to a power function, $y = a x^b$ (Fig. 8B). Using this interpolation scheme it is possible to calibrate the instrument over a fairly wide range using only two calibration points separated by

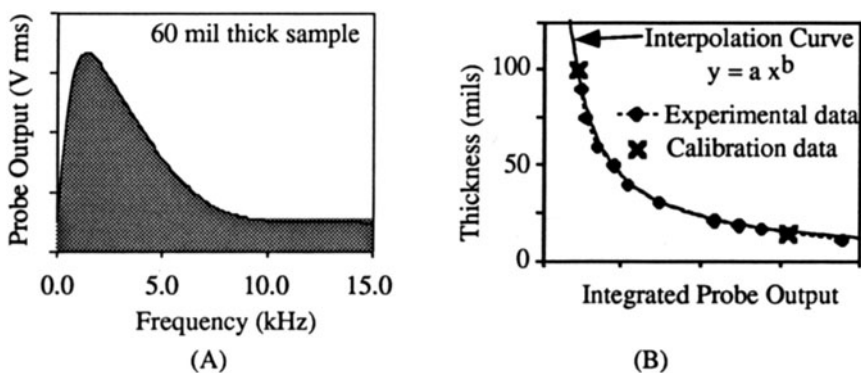


Fig. 8. (A) Frequency dependence of probe output. The area of the shaded region is used to characterize the thickness. (B) Interpolation results for the integrated probe output over a large thickness range.

a fairly large thickness variation. Thus, the user will only have to calibrate the tester on a thin and thick sample with known thicknesses and then use the values to create an interpolation curve for subsequent thickness measurements.

PERFORMANCE CHARACTERISTICS

The above algorithm was incorporated into a portable instrument (Fig.1) using an EPROM chip to perform the necessary calculations. After calibration the sensor can be used to make single or continuous thickness measurements over the range of calibration. To obtain better resolution the calibration range can be reduced. The device has been used to measure the thickness of samples ranging from 0.25mm (0.01") to 3mm (0.12") to within a tolerance of 0.013mm (0.0005").

Displayed in Fig. 9 are some typical results for a set of manufactured thickness variation samples. The samples were machined from aluminum 2024 and were 38mm (1.5") squares ranging in thickness from 0.89mm (0.035") to 1.73mm (0.068") in 0.0254mm (0.001") increments. Due to unavoidable errors in the machining process precise thickness values were not always attainable. Thickness variations on a single sample sometimes in excess of 2% of the desired thickness were quite common. In Fig. 9 we plot the relative percent error of the thickness measured by the instrument compared to the intended sample thickness. In addition, we also plot a sample thickness error. This error is based on the maximum thickness variation of a single sample as a function of the intended thickness. The maximum difference on a sample was obtained by using a micrometer to mechanically measure the samples at their centers and their four corners. The figure shows that the measured error is seldom above 2% and in those cases where the error is large the actual thickness error is also large. Thus, the actual errors are most probably within 2% of the real values. We chose to calibrate the instrument from 0.89mm (0.035") to 1.73mm (0.068") since these samples were closest to their intended values and had little sample variation.

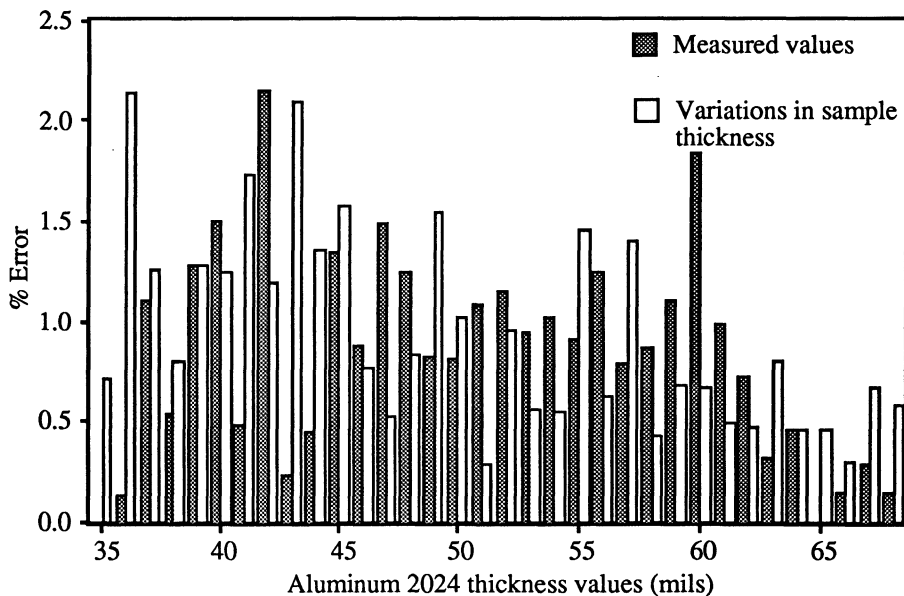


Fig. 9. Relative error of probe measurements and actual thickness as a function of sample thickness. The calibration range was from 35-68 mils.

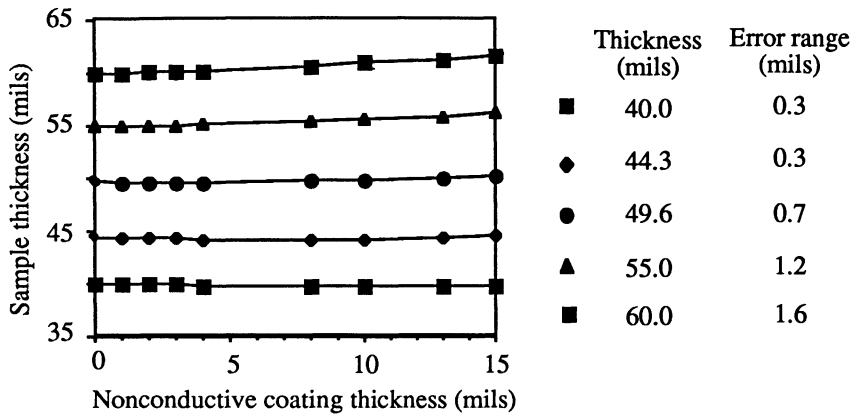


Fig. 10. Variations in probe measurements due to the presence of nonconductive coatings.

The sensor is fairly insensitive to lift-off, thus, measurements made on samples with up to 0.3mm (0.012") of a nonconductive coating, such as paint, on the surface were within 4% of their actual thickness and the results are shown in Fig. 10 below.

SUMMARY AND FUTURE DIRECTIONS

A new electromagnetic sensor and processing algorithm were used to develop a prototype thickness gauging instrument. Due to the simple interpretation and operational characteristics of the new probe it was possible to make the instrument small and portable. A nonlinear interpolation scheme incorporated into the instrument enables the user to make highly accurate thickness measurements over a fairly wide calibration range from a single side of nonferromagnetic metals. The instrument is very easy to use and can be calibrated quickly.

The capabilities of the instrument are in the process of being extended to assess corrosion in multilayer structures. At present it is possible to separate and quantify first and second layer material loss even in the presence of a variable air gap between the layers. Work continues on developing a new prototype instrument that will be able to characterize a complex multilayer structure, as is typical in the aerospace industry, which contain rivets, lap joints, stringers and surface anomalies all of which can effect the probe output.

REFERENCES

1. S. Mitra, P. S. Urali, E. Uzal, J. H. Rose and J. C. Moulder, "Eddy-Current Measurements of Corrosion-Related Thinning in Aluminum Lap Splices," *Review of Progress in Quantitative NDE*, Vol. 12B, edited by D. O. Thompson and D. E. Chimenti (Plenum Press, New York, 1993), pp. 2003-2010.
2. J. G. Thompson, "Subsurface Corrosion Detection in Aircraft Lap Splices Using a Dual Frequency Eddy Current Inspection Technique," *Materials Evaluation*, Vol. 51/Number 12 (December 1993).
3. D. J. Hagemaiier, "Eddy Current Impedance Plane Analysis," *Proceedings of the 1982 Air Transport Association Non-Destructive Testing Forum*, Atlanta, Georgia, September 14-16, 1982.
4. B. Wincheski, J. P. Fulton, S. Nath, M. Namkung and J.W. Simpson, "Self Nulling Eddy Current Probe for Surface and Subsurface Flaw Detection," *Materials Evaluation*, vol. 52, No. 1, pp. 22-26, January 1994.

5. B. Wincheski, M. Namkung, J. P. Fulton, J. Simpson and S. Nath, "Characteristics of Ferromagnetic Flux Focusing Lens in The Development of Surface/Subsurface Flaw Detector", *Review of Progress in Quantitative NDE*, Vol. 13B, edited by D. O. Thompson and D. E. Chimenti (Plenum Press, New York, 1994), pp. 1785-1792.
6. B. Wincheski, M. Namkung, J. P. Fulton and S. Nath, "New Eddy Current Probe for Thickness Gauging of Conductive Materials", *Review of Progress in Quantitative NDE*, Vol. 13B, edited by D. O. Thompson and D. E. Chimenti (Plenum Press, New York, 1994), pp.1939-1946.
7. J.P. Fulton, B. Wincheski, S. Nath and M. Namkung, "Corrosion Detection of Airframes Using a New Flux-Focussing Eddy Current Probe", Presented at the 1994 Spring conference of the American Society of Nondestructive Testing, New Orleans, LA., March 21-25, 1994.
8. M. Namkung, C.G. Clendenin, J.P. Fulton, and B. Wincheski, "An Application of a New Electromagnetic Sensor to Real-Time Monitoring of Fatigue Crack Growth in Thin Metal Plates, *Review of Progress in Quantitative NDE*, Vol. 13B, edited by D. O. Thompson and D. E. Chimenti (Plenum Press, New York, 1994), pp.1633-1640.